RESEARCH ARTICLE

Solar Cell Characteristic Studies on Metal Organic Framework/TiO_2 Hybrid Solar Cell

K. Deepak[1,*], Sampathrao L. Pinjare[2]

[1]Department of Physics, School of Applied Sciences, Reva University, Bangalore 560064, India
[2]Department of ECE, Nitte Meenakshi Institute of Technology, Bangalore 560064, India

***Corresponding author: E-mail: ukdeepak@gmail.com**

DOI: 10.5185/amlett.2020.091555

1,3,5-Triazine-2,4,6-trithiolate (TCA) coordination polymer and TiO_2 metal oxide were used to prepare a hybrid solar cell. Electrochemical polymerization of TCA on copper electrode forms CuTCA metal-organic framework (MOF). The CuTCA acts as optically active and hole transport layer whereas TiO_2 acts as exciton dissociation surface. The device was characterized under 100 mW/cm^2 condition in Cu/CuTCA-MOF/TiO_2/Ag geometry, where copper and silver serve as bottom and top electrodes respectively. The device yield power conversion efficiency (PCE) of 0.196 with open-circuit voltage (V_{oc}), short circuit current (I_{sc}) as 0.161 V and 0.431 mA/cm^2 respectively. The room temperature electrical characterization of CuTCA-MOF reveals its hole mobility (μ), thermally generated hole concentration (n_o) and resistance as 10.16x10^{-3} m^2/Vs, 8.27x10^{18} m^{-3} and 250 Ω respectively.

Introduction

The earth receives a massive amount of energy (1.75×10^{17} J) from the sun and draws attention also because it is guaranteed an alternative source of energy. However, converting this solar energy into the desired form of energy in a cost-effective way and is not an easy task. From the day when A.E. Becquerel identified the process of photovoltaic effect [**1**], the researchers working on photovoltaic technology and they succeeded in producing silicon-based solar cells. The extensive knowledge on silicon solar cells has made to use them much, but they need high purity material and vacuum deposition which increase the fabrication cost. The present research is focusing on high efficiency with low cost solar cells. Thin-film technologies have been employed for low cost solar cells, because of their solution processing technique. Preparation of most of the polymer solar cells (PSCs) employ solution processed thin film technology, because of several advantages like multilayer deposition (multi-junction), both the electron donor and acceptor layer contribute to light absorption, and reduces the cost by producing cell by a printing technique [**2**]. Especially, in case of coordination polymer, the electronic properties can be tuned by the coordination capability of functional ligands [**3**]. The high photocurrent quantum efficiency of PSCs needs more exciton close to a donor-acceptor interface where they separate into free charges and reach respective electrodes [**4**]. The serious problem in these cells is that not all generated excitons would reach the donor-acceptor interface. This is because of the exciton diffusion length in most of the polymers is 3-10 nm [**5**], which is the major obstacle for the efficiency of polymer solar cell [**6**]. A new device architecture was developed to overcome the small diffusion length of polymers called bulk heterojunction (BHJ) solar cells. These solar cells were prepared by mixing of donor and acceptor materials into an amorphous form that has different donor and acceptor regions rather than being stacked in layers in PSCs. However, the major drawback of BHJ solar cells is the large interfacial region between the donor and acceptor, which inherently increases the charge recombination and subsequently device dark current [**5**]. In the last decade, organic and inorganic materials were combined to prepare solar cells called hybrid solar cells (HSC). This versatile hybrid technique combines the advantages of inorganic semiconductors such as high carrier mobility, reliability and stability with processing flexibility of organic materials. In the hybrid (exciton) solar cells, the polymer absorbs light and creates excitons. The dissociation of generated exciton int free charges takes place near the hybrid interface. Later, new materials like perovskites and novel approaches like dye-sensitized, quantum dots solar cells were introduced to improve organic solar cell efficiency [**7**]. Similarly, coordination polymers (metal-organic framework) are new materials in the field of polymer solar cells.

Background

Understanding of working principle of hybrid solar cells is difficult than conventional silicon solar cells, because of curtail processes involved in converting light (photon) into the current (electrons). The carrier transport and recombination process are important in conventional cells. In addition to these two-process exciton transport, recombination and dissociation are crucial processes in hybrid solar cells; here the focus is on the excitons themselves. An exciton is nothing but a bound state of an

electron and hole, which are held together by the electrostatic Coulomb force. The energy level relationships of a typical bilayer HSCs are shown in **Fig. 1** [**8**]. The optical band gap is the energy threshold for photons to be absorbed by creating exciton in the organic semiconductor, while the electrical bandgap is the threshold (or minimal energy required) to create an electron-hole pair which is not bound together. The difference between the optical band gap and the electrical bandgap is the exciton binding energy. The optical band gap energy is at lower than electrical bandgap energy because of the low dielectric constant that is typical of organic materials and because of the weak intermolecular electronic interactions (small Bohr radius of carriers) [**8**]. These two effects result in the self-trapping of the initial charge carrier in the Coulomb field of its conjugate carrier, producing a singlet exciton upon light absorption. The thermodynamic requirement for an exciton to dissociate at an interface is that the band offset must be greater than the exciton binding energy (**Fig. 1**).

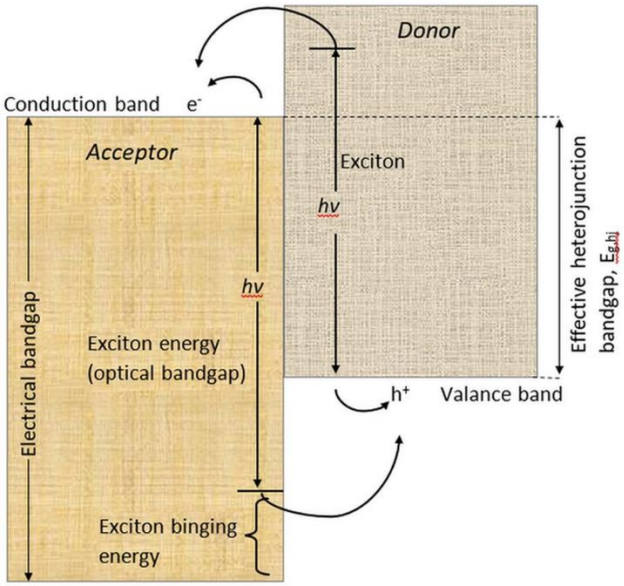

Fig. 1. Energy-level diagram for a hybrid (excitonic) solar cell. Excitons in donor do not have enough energy to dissociate in the bulk, but the offset of conduction and valence bands at the interface between acceptor and donor polymers provide an exothermic pathway for dissociation of excitons into free charge carriers.

The combination of metal oxide (e.g., TiO_2, ZnO, Al_2O_3) and the conjugated polymer is an attractive donor-acceptor pair candidate in excitonic solar cells. Generally, semiconductor metal oxides are categorized under thin films and are used as an electron transport layer between the organic layer and the electrode (cathode). This group of materials have grabbed the interest of researchers because they can be prepared in a wide range of morphologies. By the control of morphology via wet chemical synthetic technique, a material can be prepared as a dense film to rigidly connected nanostructures to dispersed nanocrystals, offering a valuable perception into the role of morphology in the photovoltaic action. Furthermore, metal oxides offer good optical properties which enhance light absorption, they are cheap and non-toxic and enjoy a large experience base from research into photocatalysis, gas sensors, and dye-sensitized solar cells. Titanium dioxide (TiO_2) has been widely studied for hybrid organic-inorganic solar cells. It is known that TiO_2 is intrinsically n-type semiconductor with high electron affinity, which stems from the position of its conduction bands and enables it to match with the LUMO of most of the organic semiconductors [**9**]. It offers good Ohmic contact to both donors and acceptors in polymer solar cells and shown as a promising acceptor material in hybrid solar cells [**10, 11**]. Its wide bandgap of about 3.2 eV made the TiO_2 as transparent semiconducting metal oxide to visible as well as infrared, therefore it is insensitive to visible and infrared light, which permits it to absorb ultraviolet region of the solar spectrum [**12**].

Conjugated polymers are used to fabricated polymer solar cells, they yielded low power conversion efficiencies due to limited interfacial contact area between the donor and acceptor layers, low mobility, high resistivity etc. Coordination polymers (CPs) have concerned a great deal of consideration in a variety of scientific fields due to their novel and fascinating structural properties. CPs means compounds in which metal entities linked by inorganic ligands, both metal ions and coordinating groups occur as regularly repeating units, these are also termed as metallopolymers or metal-organic frameworks (MOFs) [**13**]. MOFs have been investigated for a wide range of applications like photocatalysis, gas storage, catalysis, photoluminescence-based sensors, and drug delivery etc. [**14**]. The combination of a wide range of metal ions and a variety of organic ligands tailor the desired properties of MOFs to be conveniently tuned vis-à-vis a particular application. The bandgap engineering and light-harvesting capacity of MOFs can be done through rational functionalization of the linking unit, they have an extraordinarily large internal surface area due to their porous structure [**14**]. Lately, the investigation into MOFs for photovoltaic processes has become one of the most exciting research avenues for the development of future solar cells. In this work, the MOF is formed using TCA ($C_3N_3S_3$) as bridging ligand with copper (Cu) metal ions (Cu ions containing polymer, CuTCA) [**13**]. The simple method of preparation of CuTCA MOF by electrochemical polymerization is explained in the early report [**15**]. This CuTCA thin-film cathode is a visible light active and is a p-type semiconductor with high conductivity [**16**]. In this proposed work we have prepared a hybrid solar cell using CuTCA MOF. To the best of our knowledge, this is the first report on CuTCA MOF used for photovoltaic application.

Experimental

CuTCA film deposition

1,3,5-Triazine-2,4,6-trithiol trisodium salt solution (15%) is procured from Sigma-Aldrich and copper (Cu) foils were used to prepare CuTCA MOF thin films by electrochemical deposition [**15**]. Copper foils of thickness ~ 0.1 mm and

geometrical area of 1 cm^2 were polished with emery, washed with deionized water, then dried at room temperature. Three-electrodes electrochemical cell having Pt as a counter, Cu as a working and Ag/AgCl in 0.1 M KCl, as a reference electrode was used for polymerization of TCA on Cu which forms CuTCA MOF. Electrochemical anodization was performed by applying an open-circuit voltage of 50 mV for 5 min. The scheme of multilayer deposition of CuTCA is shown in **Fig. 2** and its detailed growth is discussed in the earlier report [**15**]. The CuTCA on Cu electrodes is washed with Millipore water and dried for further process.

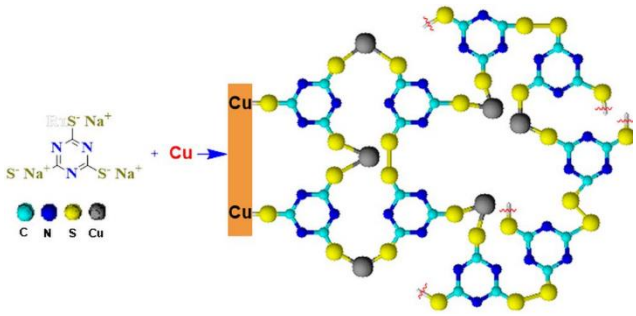

Fig. 2. Scheme of multilayer deposition of CuTCA MOF.

Preparation of solar cell

The TiO_2 colloidal solution was prepared by adding 0.2 g of TiO_2 nanopowder of 25nm particle size to the mixture of 0.5 ml deionized water and 0.2 ml of 0.05 M HNO_3 solution, then the solution was stirred at 120 rpm at room temperature until a uniform homogenous paste is formed [**17**]. TiO_2 paste was spin-cast on early prepared CuTCA electrode at 2000 rpm for 60 sec, annealed at 80°C for 10 min. The silver (Ag) contacts were given on the TiO_2 layer to get the devices structures as Cu/CuTCA/TiO_2/Ag as shown in **Fig. 3(a)**. The energy level diagram (not to scale) of the solar cell is presented on the basis DC characteristics of CuTCA which explains the working of the device as shown in **Fig. 3(b)**. The typical device area is ~1 cm^2 and thickness is approximately ~3.5 µm.

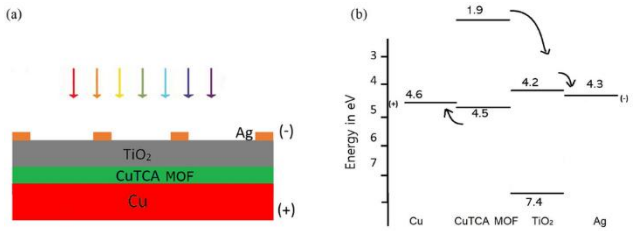

Fig. 3. (a) Side view of Cu/CuTCA MOF/TiO_2/Ag solar cell. (b) The energy level diagram which explains the working principle of the solar cell.

Result and discussion

Bandgap and thickness measurement

Energy Bandgap engineering is one of the emerging and challenging research in semiconductors. The application potential of any material is characterized by bandgap energy (E_g). Bandgap estimation is most significant in material characterization because most of the electrical behaviour and optical properties of semiconductors are well explained by bandgap as well as energy levels (HOMO & LUMO) also. The E_g of the material can be found by UV-Vis-NIR absorption spectroscopy and Diffuse Reflectance Spectroscopy (DRS). DRS technique is used in this work because the polymer is coated on nontransparent material (copper). In DRS, the reflectance is calculated by the Kubelka-Munk (KM) equation $(k/s = (1-R)^2/2R)$ [**18**].

Where *R* is the *KM* function (absolute diffuse reflectance), *k* is the absorption coefficient and *s* is the scattering coefficient. In DRS the absorption can be calculated from a plot $[k/s*hv]^2$ along y-axis and *hv* along the x-axis [**19,20**]. The bandgap of the material is obtained by extrapolating a straight line as shown in **Fig. 4(a)** and the bandgap of CuTCA is found to be ~2.6 eV. The thickness of the CuTCA film is about ~1.5 µm, which is seen in the cross-sectional FESEM image as shown in **Fig. 4(b)**.

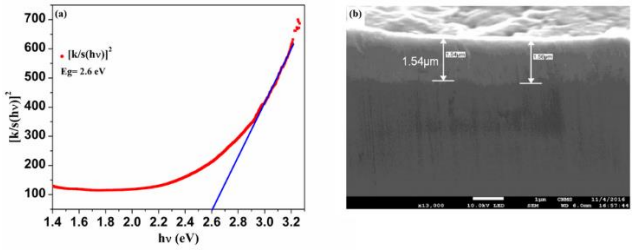

Fig. 4. (a) Kubelka-Munk $[(k/s*hv)^2$ *vs hv]* plot from DRS to find the bandgap of CuTCA and obtained bandgap value is 2.6 eV. (b) Cross view of FESEM image of the CuTCA film.

Electric characterization of CuTCA

The current-voltage *(I-V)* characteristic of CuTCA was recorded in Cu/CuTCA/Ag sandwich geometry as shown in the **Fig. 5(a)**. Keithley 2450 was used to apply the voltage across the sample (sweep from -0.5 V to 0.5 V) and measure the current through the sample at room temperature. **Fig. 5 (b)** uncovers the completely absent of Schottky barrier with both the electrodes by the polymer because the *I-V* curve is symmetrical in both forward and reverse bias [**21**]. In forward bias (Cu electrode being positively biased), the slope of a log I vs log V plot is equal to ~1 as shown in **Fig. 5(c)**, which is the characteristic of Ohmic (linear) conduction, and this behaviour is described by Ohm's law [**22**].

$$J_{ohm} = n_o q \mu V/d \quad (1)$$

where n_o is the thermally generated hole concentration, q is the electronic charge, μ is the hole mobility, V is the applied voltage, and d is the thickness of the polymer (or electrode separation). The temperature-dependent electrical characterization of CuTCA is reported in early work where the transition from ohmic conduction to space charge-limited conduction (SCLC) takes place at 200 K at 0.1 V called crossover voltage (V_t) [**16**]. At crossover voltage, the injected carrier concentration first exceeds the thermally generated carrier concentration called SCLC.

The thermally generated hole concentration (n_o) is calculated as 8.27x10^{18} m^{-3}, using the relation [**23**],

$$V_t = \frac{8en_0d^2}{9\varepsilon_r\varepsilon_0} \quad (2)$$

where ε_r is the relative permittivity of the material, ε_0 is the permittivity of free space (8.825 x 10^{-12} F/m). V_t is the crossover (transition) voltage. From Eq. (1) the hole mobility is calculated as 10.16x10^{-3} m^2/Vs. The resistance value of the polymer from *I-V* is 250 Ω.

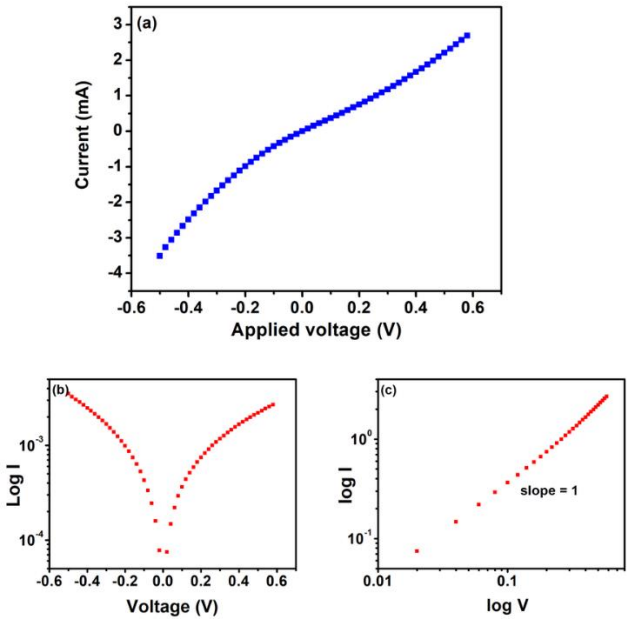

Fig. 5. (a) Current-voltage characteristic curve in Cu/CuTCA/Ag geometry. (b) I-V curves under forward and reverse biases. (c) log I vs log V plot with slope ~1, showing Ohmic conduction.

Solar cell characterization

The solar cell was characterized using a homemade sample holder having 450 W xenon lamp. The current-voltage measurements were carried out by Bio-Logic SP-300 potentiostat which is controlled by a computer. The solar radiation was illuminated on the cell through TiO_2. The excitons get generated near the polymer/TiO_2 heterointerface in short circuit condition. The generated excitons diffuse towards interface where it dissociates into free charge carriers by the built-in voltage (without considering any surface interactions and defects) [**2**]. The electrons are collected in Ag and holes in the Cu electrodes. The working principle of the proposed cell made of CuTCA MOF and TiO_2 is schematically shown in **Fig. 3(b)**. The I-V measurements were carried out to extract solar cell parameters such as open-circuit voltage (V_{oc}), short circuit current (I_{sc}) is shown in **Fig. 6**. The other parameters of the solar cell are tabulated in **Table 1**.

Table 1. Measured photovoltaic parameters of Cu/CuTCA MOF/TiO_2/Ag solar cell.

Voc (V)	Jsc (mA/cm^2)	Vmp (V)	Imp (mA/cm^2)	FF (%)	η (%)
0.161	0.431	0.101	0.194	28.2	0.196

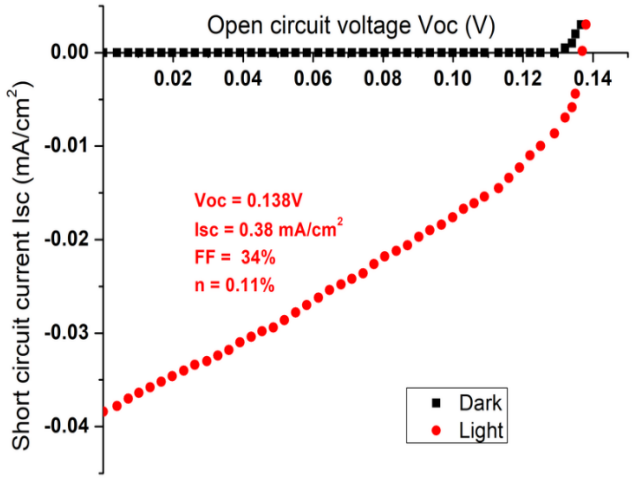

Fig. 6. Current-voltage characteristics of the solar cell.

The V_{oc} is the voltage for which the current in the external circuit is zero. 0.161 V is the value of V_{oc} from I-V curve. The electronic bandgap between donor-acceptor polymer defines the Voc in the hybrid solar cell [**8**]. The electronic bandgap value depends on the potential energy of the electrons which are in the conduction band (CB) of the acceptor and the holes in the highest occupied molecular orbital (HOMO) of the donor (E^D_{HOMO} - E^A_{LUMO} = ideal value). According to the energy level diagram of propose cell, the value of Voc is 0.3 V but from the I-V curve, it is 0.161 V which is less than the ideal value because of several factors. In real Voc depends on many factors like carrier recombination, traps in the polymer, dipoles formation in the interface, modification of work functions of electrodes [**11,24-30**]. The proper tuning of HOMO/CB gap between polymer-metal oxide would increase the open-circuit voltage.

The current which flows in the solar cell when it is short-circuited is known as short circuit current (I_{sc}). The amount of photogenerated carriers decides the short circuit current. I_{sc} of a polymer solar cell mainly depends on the light spectrum absorption capacity, mobility, traps, bandgap of polymers [**31**]. The measure I_{sc} of the proposed solar cell is 0.431 mA/cm^2. I_{sc} can be increased by increasing the light absorption capacity of polymer which intern increases the efficiency of the solar cell [**32**].

The shape of the I-V curve is decided by the fill factor (FF), which is the ratio between the maximum power output of a cell (P_{mp}) to the product of open-circuit voltage and short circuit current (FF = P_{mp} / V_{oc}*I_{sc}). The fill factor depends on the V_{oc} and I_{sc}. The calculated FF of the proposed solar cell is 28.2%. The solar cell is measure by its power conversion efficiency (PCE) under the light. The PCE is calculated by η = (V_{oc}*I_{sc}*FF) / Pin and optimized product of V_{oc}, I_{sc} and FF increase the efficiency of a cell. The calculated value of PCE of the proposed solar cell is 0.196%.

Conclusion

This work was dedicated to study the photovoltaic behaviour of hybrid solar cell made by CuTCA MOF and TiO_2 metal oxide. 1,3,5-Triazine-2,4,6-trithiol trisodium salt (TCA) was coated on Cu foils which forms CuTCA metal-organic framework (MOF) by electrochemical methods. TiO_2 was spin-coated on early prepared CuTCA, finally, silver contacts were made to get Cu/CuTCA-MOF/TiO_2/Ag geometry. The characterization of the solar cell shown 0.196 % efficiency with V_{oc} and I_{sc} as 0.161 V and 0.431 mA/cm^2 respectively. The room temperature I-V measurements of CuTCA-MOF reveals its hole mobility *(μ)*, thermally generated hole concentration *(n_o)* and resistance as 10.16x10^{-3} m^2/Vs, 8.27x10^{18} m^{-3} and 250 Ω respectively.

Keywords

Metal organic framework, Coordination polymer, Hybrid solar cell, electrochemical deposition, dc characterization.

Received: 18 March 2020
Revised: 21 April 2020
Accepted: 04 May 2020

References

1. A. E. Becquerel.; *Compt. Rend. Acad. Sci.*, **1839**, *9*, 561.
2. Moul, A.J.; Chang, L.; Thambidurai, C.; Vidu, R.; Stroeve, P.; *J. Mater. Chem.*, **2012**, *22*, 2351.
3. Gonzalo G.; Amo-Ochoa, P.; Carlos, J.G.; Felix, Z.; *Chem. Soc. Rev.* **2012**, *41*, 115.
4. Boucle, J.; Ravirajan, P.; Nelson, J.; *J. Mater. Chem.*, **2007**, *17*, 3141.
5. Goh, C.; Scully, S.R.; Mcgehee, M.D.; *J. Appl. Phys.*, **2007**, *101*, 114503.
6. Bernède, J.C.; *J. Chil. Chem. Soc.*, **2008**, *53*, 1549.
7. Oseni, S.O.; Mola, G.T.; *Sol. Energy Mater. Sol. Cells.*, **2017**, *160*, 241
8. Gregg, B.A.; *MRS bulletin*, **2005**, *30*, 20.
9. Anitha, V.C.; Banerjee, A.N.; Sang W. J.; *J. Mater. Sci.*, **2015**, *50*, 7495.
10. Abayev, I.; Zaban, A.; Fabregat-Santiago, F.; Bisquert, J.; *Phys. Stat. Sol. (A).*, **2003**, *196*, 5.
11. Chen, S.; Manders, J.R.; Tsang, S.W.; So, F.; *J. Mater. Chem.*, **2012**, *22*, 24202.
12. Herz, L.M.; Tiwana, P.; Snaith, H.J.; Docampo, P.; Johnston, M.B.; *ACS Nano.*, **2011**, *5*, 5158
13. Chudy, J.C.; Dalziel, J.A.W.; *J. inorg. nucl. Chem.*, **1975**, *37*, 2459.
14. Kaur, R.; Kim, K.-H.; Paul, A.K.; Deep, A.; *J. Mater. Chem. A.*, **2016**, *4*, 3991.
15. Vishwanath, R.S.; Kandaiah, S.; *J. Electrochem. Soc.*, **2016**, 163, H402.
16. Deepak, K.; Roy, A.; Anjaneyulu, P.; Kandaiah, S.; Pinjare, S.L.; *J. Appl. Phys.*, **2017**, *122101*, 164504.
17. Kishore Kumar, D.; Hsu, M.H.; Ivaturi, A.; Chen, B.; Bennett, N.; Upadhyaya, H.M.; *Flex. Print. Electron.* **2019**, *4*, 015007.
18. Murphy, A.B.; *Sol. Energy Mater. Sol. Cells.*, **2007**, *91*, 1326.
19. Aneesh, P.M.; Krishna, K.M.; Jayaraj, M.K.; *J. Electrochem. Soc.* **2009**, *156*, 33.
20. Mola, G.T.; Arbab, E.A.A.; Taleatu, B.A.; Kaviyarasu, K.; Ahmad, I.; Maaza, M.; *J. Microsc.* **2017**, *265*, 214.
21. Kronemeijer, A.J.; Huisman, E.H.; Katsouras, I.; Van Hal, P.A.; Geuns, T.C.T.; Blom, P.W.M.; Van Der Molen, S.J.; De Leeuw, D.M.; *Phys. Rev. Lett.*, **2010**, *105*, 156604.
22. Chiguvare, Z.; Parisi, J.; Dyakonov, V.; *J. Appl. Phys.* **2003**, *94*, 2440.
23. Gould, R.D.; *Coordin. Chem. Rev.*, **1996**, *156*, 237.
24. Gregg, B.A.; *J. Phys. Chem.*, **2003**, *107*, 4688.
25. Brabec, B.C.J.; Cravino, A.; Meissner, D.; Sariciftci, N.S.; Fromherz, T.; Rispens, M.T.; Sanchez, L.; Hummelen, J.C.; *Adv. Funct. Mater.*, **2001**, *11*, 374.
26. Heller, C.M.; Campbell, I.H.; Smith, D.L.; Barashkov, N.N.; Ferraris, J.P.; *J. Appl. Phys.*, **1997**, *81*, 3227.
27. Mihailetchi, V.D.; Koster, L.J.A.; Blom, P.W.M.; *Appl. Phys. Lett.*, **2004**, *85*, 970.
28. Hoppe, H.; Sariciftci, N.S.; *J. Mater. Res.*, **2004**, *19*, 1924.
29. Frohne, H.; Shaheen, S.E.; Brabec, C.J.; Müller, D.C.; Sariciftci, N.S.; Meerholz, K.; *ChemPhysChem.*, **2002**, *3*, 795.
30. Mihailetchi, V.D.; Blom, P.W.M.; Hummelen, J.C.; Rispens, M.T.; *J. Appl. Phys.*, **2003**, *94*, 6849.
31. Lee, H.; Lee, C.; Song, H.J.; *Materials*, **2019**, *12*, 1.
32. Wanninayake, A.P.; Gunashekar, S.; Li, S.; Church, B.C.; Abu-Zahra, N.; *Semicond. Sci. Technol.*, **2015**, *30*, 1.